Inorganic Chemistry

Article

pubs.acs.org/IC

Phosphorus Complexes of *meso*-Triaryl-25-oxasmaragdyrins

Hemanta Kalita,[†] Way-Zen Lee,[‡] and Mangalampalli Ravikanth*,[†]

[†]Department of Chemistry, Indian Institute of Technology, Powai, Mumbai 400076, India

[‡]Instrumentation Center, Department of Chemistry, National Taiwan Normal University,88 Section 4 Ting-Chow Road, Taipei 11677, Taiwan

Supporting Information

ABSTRACT: The aromatic PO_2 complexes of *meso*-triaryl-25-oxasmaragdyrins were synthesized by treating the free base 25-oxasmaragdyrins with $POCl_3$ in toluene/triethylamine at refluxing temperature. The complexes are stable and characterized by X-ray and different spectroscopic techniques. In these complexes, the phosphorus(V) ion was bound to two pyrrolic nitrogen atoms of the smaragdyrin macrocycle and two oxygen atoms in tetrahedral geometry. The X-ray structure revealed that the smaragdyrin macrocycle showed significant distortion upon insertion of a PO_2 unit, and the phosphorus atom lies 1.339 Å above the mean plane defined by three *meso*-carbon atoms of the macrocycle. These complexes absorb strongly in the visible region and are 2.5 times more strongly fluorescent than free base 25-oxasmaragdyrins. The smaragdyrin macrocycle becomes electron-deficient upon complexation with a PO_2 unit because these complexes are easier to reduce but difficult to oxidize compared to free base smaragdyrins. We designed and synthesized a covalently linked BODIPY−PO_2-smaragdyrin dyad and demonstrated efficient energy transfer from the BODIPY unit to the PO_2-smaragdyrin unit.

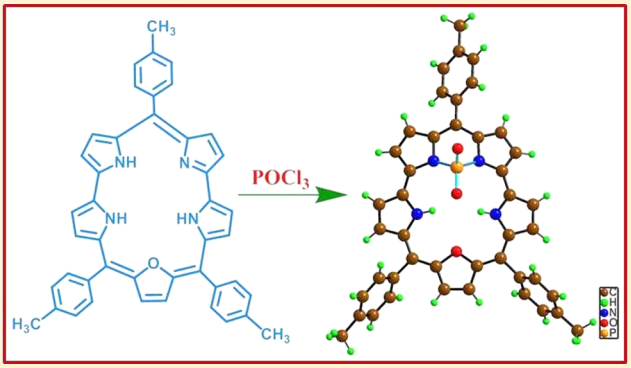

INTRODUCTION

Sapphyrins and smaragdyrins are pentapyrrolic 22π-electron macrocyclic cousins and differ from each other in the number of bridging carbon atoms and direct bonds that connect the five pyrrole rings.[1] Sapphyrins contain one direct pyrrole−pyrrole bond, whereas the smaragdyrins contain two direct pyrrole−pyrrole bonds.[1] Sapphyrins were the first stable expanded porphyrins reported in the literature and have remained some of the most extensively studied macrocycles.[2] The strategies used to synthesize sapphyrins are well established, and these macrocycles are versatile anion-binding agents. They possess rich porphyrin-like coordination chemistry[3] and have been used for diverse applications. Although smaragdyrins were discovered at the same time as sapphyrins,[4] the chemistry of smaragdyrins remained underdeveloped because of the lack of proper synthetic protocols, difficulties in accessing the desired stable precursors, and their own unstable nature. Earlier workers attempted to synthesize stable *meso*-free β-substituted smaragdyrins,[5] but the chemistry was not explored to a greater extent because of their instability. In fact, to the best of our knowledge, there is no report on *meso*-triarylpentaazasmaragdyrin indicating the unstable nature of the macrocycle. In 1999, Chandrashekar and co-workers reported the first stable *meso*-triaryl-25-oxasmaragdyrin by trifluoroacetic acid (TFA)-catalyzed oxidative coupling of *meso*-aryldipyrromethane with 16-oxatripyrrane and studied their anion- and metal-binding properties.[6,7] 25-Oxasmaragdyrins absorb and emit in the red region with decent extinction coefficients and quantum yields and are stable under redox conditions. Chandrashekar and co-workers also showed the coordinating ability of 25-oxasmaragdyrins by synthesizing rhodium(I) and nickel(II) complexes and explored their properties.[7] We recently found that BF_2-complexation of 25-oxasmaragdyrin resulted in significant alteration of its properties such as 3 times enhancement in the intensity of the absorption band at ∼700 nm, higher quantum yields, and low reduction potentials compared to free base smaragdyrins.[8] We also prepared $B(OR)_2$ complexes of smaragdyrin and studied their spectral, photophysical, and electrochemical properties.[9] This encouraged us to test the coordinating ability of 25-oxasmaragdyrins toward main-group elements such as phosphorus. It is well established in the literature that tetrapyrrolic macrocycles such as porphyrin,[10] corrole,[11] and N-fused porphyrin[12] readily bind with phosphorus, and the representative examples of these systems are shown in Chart 1 (**I**−**III**). Interestingly, there are only three reports on phosphorus complexes of expanded porphyrinoids such as expanded isopholorin, [28]octaphyrin,[13] [30]-hexaphyrin,[14] and triply fused [24]pentaphyrin.[15] In all of these reported phosphorus complexes of expanded porphyrinoids,[13−15] the expanded porphyrinoid is bound to one or two phosphorus atom(s) via a combination of pyrrolic nitrogen, pyrrolic β-carbon, and oxygen atoms, as shown for bisphosphorus octaphyrin complex **IV** (Chart 1). Thus, the

Received: July 9, 2014
Published: August 18, 2014

   dx.doi.org/10.1021/ic501629n | *Inorg. Chem.* 2014, 53, 9431−9438

Chart 1. Reported Phosphorus Complexes of Porphyrin (I), Corrole (II), N-Fused Porphyrin (III), and Expanded Porphyrinoid (IV)

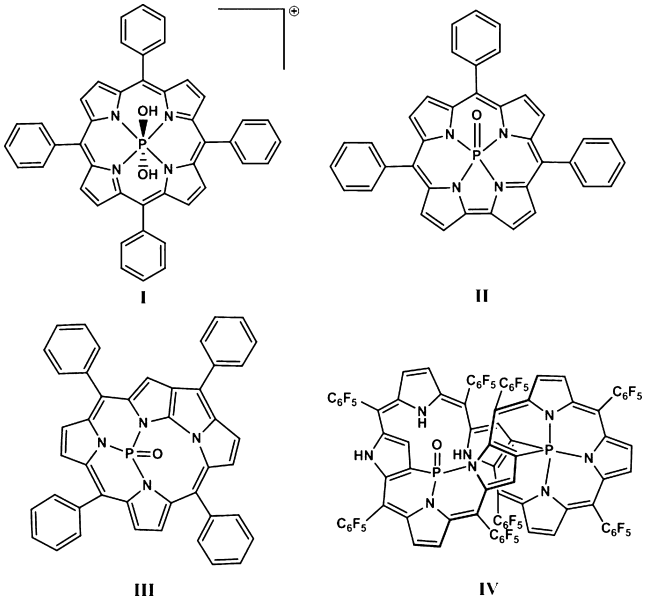

reports on phosphorus complexes of expanded porphyrinoids are very limited to understand their physicochemical properties in detail. Herein we report the fluorescent phosphorus complexes of *meso*-triaryl-25-oxasmaragdyrin **1**–**4** in which phosphorus(V) was bound to two pyrrolic nitrogen atoms of the dipyrromethene moiety of 25-oxasmaragdyrin and two oxygen atoms in unique tetrahedral geometry. The PO_2 complexes are aromatic, decently fluorescent, and stable under redox conditions. Furthermore, to show the use of PO_2-smaragdyrin as an efficient energy acceptor, we synthesized a covalently linked BODIPY–PO_2-smaragdyrin dyad and our steady-state fluorescence studies indicated an efficient energy transfer from the BODIPY unit to the PO_2-smaragdyrin unit upon selective excitation of the BODIPY unit.

RESULTS AND DISCUSSION

PO_2-Smaragdyrin Complexes 1–4. The free base *meso*-triarylsmaragdyrins **5**–**8** were prepared following the literature procedure.[6] The phosphorus insertion into *meso*-arylsmaragdyrin **5** was tested with PCl_3, PBr_3, and $POCl_3$ as phosphorylating reagents. The *meso*-triarylsmaragdyrin **5** was treated with an excess of phosphorylating reagents in toluene/NEt_3 at refluxing temperature, and the progress of the reaction was followed by thin-layer chromatography (TLC) analysis and UV–vis spectroscopy at frequent intervals (Scheme 1). The color of the reaction mixture changed from green to brownish green only in the presence of $POCl_3$, and no change in the color was observed with the other two reagents. TLC analysis also indicated the progress of the reaction by showing a bright-green polar spot along with a less polar spot corresponding to the unreacted free base smaragdyrin in the case of the $POCl_3$ reaction and no indication of the formation of product in the case of the other two reagents. Absorption spectroscopy also indicated the formation of a phosphorus-inserted smaragdyrin complex. Thus, the initial studies clearly indicated that $POCl_3$ is a suitable phosphorylating reagent for smaragdyrin. The crude compound was subjected to silica gel column chromatography using petroleum ether/CH_2Cl_2, and the desired compound **1** was collected as a fluorescent green band in 55% yield. Compounds **2**–**4** were also prepared by treating the corresponding free base smaragdyrins **6**–**8**, respectively, under similar reaction conditions (Scheme 1). Compounds **1**–**4** were freely soluble in common organic solvents and were characterized by high-resolution mass spectrometry (HR-MS), NMR, absorption, fluorescence, and electrochemical techniques. HR-MS analysis clearly indicated that a PO_2 unit was complexed with a smaragdyrin macrocycle. The formation of PO_2 complexes of 25-oxasmaragdyrins **1**–**4** was also unambiguously confirmed by detailed 1D and 2D NMR studies

Scheme 1. Synthesis of PO_2-oxasmaragdyrin Complexes 1–4

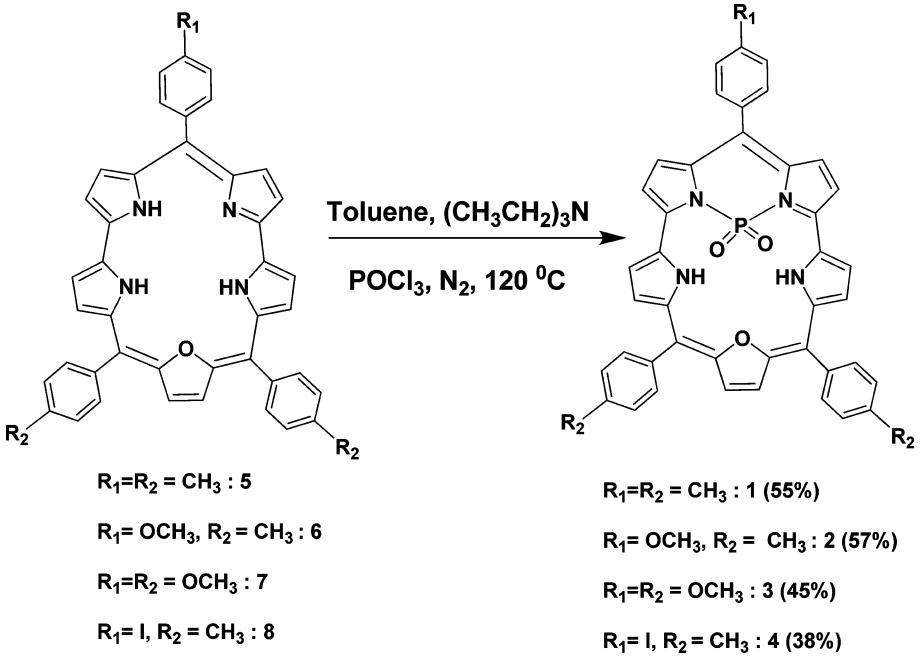

dx.doi.org/10.1021/ic501629n | Inorg. Chem. 2014, 53, 9431–9438

(Supporting Information, S1 and S2). Furthermore, compound **1** was characterized by X-ray crystallography.

Crystallographic Studies of Compound 1. The X-ray structure solved for compound **1** (CCDC 975030) confirmed the formation of a PO_2 complex of smaragdyrin **1**. The crystal suitable for X-ray diffraction analysis was obtained by vapor diffusion of *n*-hexane into a solution of compound **1** in chloroform over a period of 10 days. Compound **1** was crystallized in triclinic space group $P\bar{1}$, and the relevant crystallographic data are presented in Table 1. The crystal

Table 1. Crystallographic Data of Compound 1

parameters	compound **1**
molecular formula	$C_{44}H_{33}N_4O_3P$
fw	696.71
cryst syst	triclinic
space group	$P\bar{1}$
a (Å)	8.7643(5)
b (Å)	11.0201(8)
c (Å)	20.4623(18)
α (deg)	79.730(5)
β (deg)	80.208(5)
γ (deg)	89.199(6)
V (Å^3)	1916.1(2)
Z	2
μ (mm^{-1})	0.116
D_{calcd} (g cm^{-3})	1.208
$F(000)$	728
2θ range (deg)	1.88−25.04
indep reflns	6724 [R(int) = 0.0569]
R1, wR2 [$I > 2\sigma(I)$]	0.0698, 0.1887
R1, wR2 (all data)	0.1024, 0.2071
GOF	1.071
largest diff peak, hole (e Å^{-3})	0.336, −0.326

structure of compound **1** is shown in Figure 1, and the selected bond lengths and angles are presented in Table 2. The crystal structure revealed that the smaragdyrin macrocycle in compound **1** is not planar. PO_2 unit complexation with the smaragdyrin macrocycle resulted in significant distortion of the macrocycle. The phosphorus atom lies 1.339 Å above the mean plane defined by three *meso*-carbon atoms of the macrocycle. The phosphorus(V) atom was bound to two pyrrolic nitrogen atoms, N1 and N2, of the dipyrrin moiety and two oxygen atoms in a tetrahedral fashion. The two pyrrole rings I and II that were bound to the PO_2 unit were more deviated upward by 0.34 Å (13.72°) and 0.26 Å (21.78°), respectively, whereas the other three heterocyclic rings, III, IV, and V, that were not bound to the PO_2 unit were less deviated from the mean plane. Furthermore, it is also clear from the structure that one of the oxygen atoms of the PO_2 unit was involved in very strong intramolecular hydrogen bonding with the inner NH atom. The oxygen atom of the furan moiety of compound **1** also showed weak intramolecular hydrogen bonding (Supporting Information, S25) with the same inner NH atoms (Table 2). The packing diagram showed that both oxygen atoms of the PO_2 unit were involved in intermolecular hydrogen bonding; one of the oxygen atoms of the PO_2 moiety was involved in hydrogen bonding with one of the hydrogen atoms of the *meso*-tolyl $-CH_3$ group and the second oxygen atom was involved with the hydrogen atoms of the phenyl ring of an adjacent molecule (Supporting Information, S24), thus leading to the 3D-supramolecular architecture.

Spectral and Electrochemical Studies of Compounds 1−4. The absorption properties of PO_2 complexes of smaragdyrins **1**−**4** were studied in a choloroform solvent and compared with free base smaragdyrin **5** (Table 3). The comparison of absorption spectra of a PO_2 complex of smaragdyrin **1** with its corresponding free base smaragdyrin **5** is shown in Figure 2. The free base smaragdyrin **5** show four Q bands at 555, 600, 636, and 699 nm and one Soret band at 447 nm in the absorption spectrum. However, in complexes **1**−**4**, the absorption bands were significantly shifted bathochromically with increases in the extinction coefficients. Especially, complex **1** differs from the free base smaragdyrin **5** in the Soret region where complex **1** showed two distinct well-separated bands at 448 and 486 nm, unlike one broad band observed for free base smaragdyrin **5**. Furthermore, the Q-band region of complex **1** showed a strong band at 708 nm (Figure 2), which is 3 times more intense than the absorption band of free base smaragdyrin **5** in the same region.

The electrochemical properties of PO_2 complexes **1**−**4** along with free base smaragdyrin **5** are followed by cyclic voltammetry (CV) and differential pulse voltammetry (DPV) in CH_2Cl_2 using tetrabutylammonium perchlorate (TBAP) as the supporting electrolye. The representative cyclic voltammogram of the PO_2 complex **1** is shown in Figure 3, and the relevant redox data are presented in Table 4. In general, a free base smaragdyrin such as compound **5** shows two reversible/quasi-reversible oxidations and two irreversible reductions, indicating that the smaragdyrin macrocycle is not stable under redox conditions. As cleared from Figure 3, the PO_2 complexes such as **1** show two reversible oxidations at 0.74 and 1.12 V, one reversible reduction at −0.92 V, and one quasi-reversible reduction at −1.50 V (Figure 3), indicating that the PO_2 complexes **1**−**4** are stable under redox conditions. The oxidation potentials of the PO_2 complexes **1**−**4** were shifted toward more positive and the reduction potentials toward less negative compared to free base 25-oxasmaragdyrin **5**, indicating that complexes **1**−**4** are difficult to oxidize but easier to reduce (Table 4). Thus, it is observed that PO_2 complexation makes the resulting smaragdyrin macrocycle more electron-deficient than the free base smaragdyrin.

The fluorescence properties of complexes **1**−**4** were studied by both steady-state and time-correlated single photon counting (TCSPC) techniques in a chloroform solvent. The comparison of fluorescence spectra of the PO_2-smaragdyrin complex **1** with the free base smaragdyrin **5** is shown in Figure 4, and the relevant data are included in Table 3. The free base 25-oxasmaragdyrin **5** showed one broad fluorescence band at 710 nm with a singlet-state quantum yield of 0.07. The PO_2 complexes **1**−**4** are relatively more fluorescent than free base smaragdyrins and exhibited a slightly bathochromically shifted fluorescence band in the 714−720 nm region with a quantum yield of 0.13−0.18 (Table 3). The singlet-state lifetimes of PO_2 complexes were measured by time-resolved fluorescence studies, and the representative fluorescence decay profile of compound **1** in $CHCl_3$ collected at the corresponding emission maxima wavelength is shown in Figure 5. The fluorescence decay profiles of compounds **1**−**4** were fitted as single-exponential, and the singlet-state lifetimes observed were in the range of 3.9−4.3 ns. The singlet-state lifetimes of the PO_2 complexes **1**−**4** were slightly higher than the free base smaragdyrin, and these lifetimes are parallel to the fluorescence

dx.doi.org/10.1021/ic501629n | Inorg. Chem. 2014, 53, 9431−9438

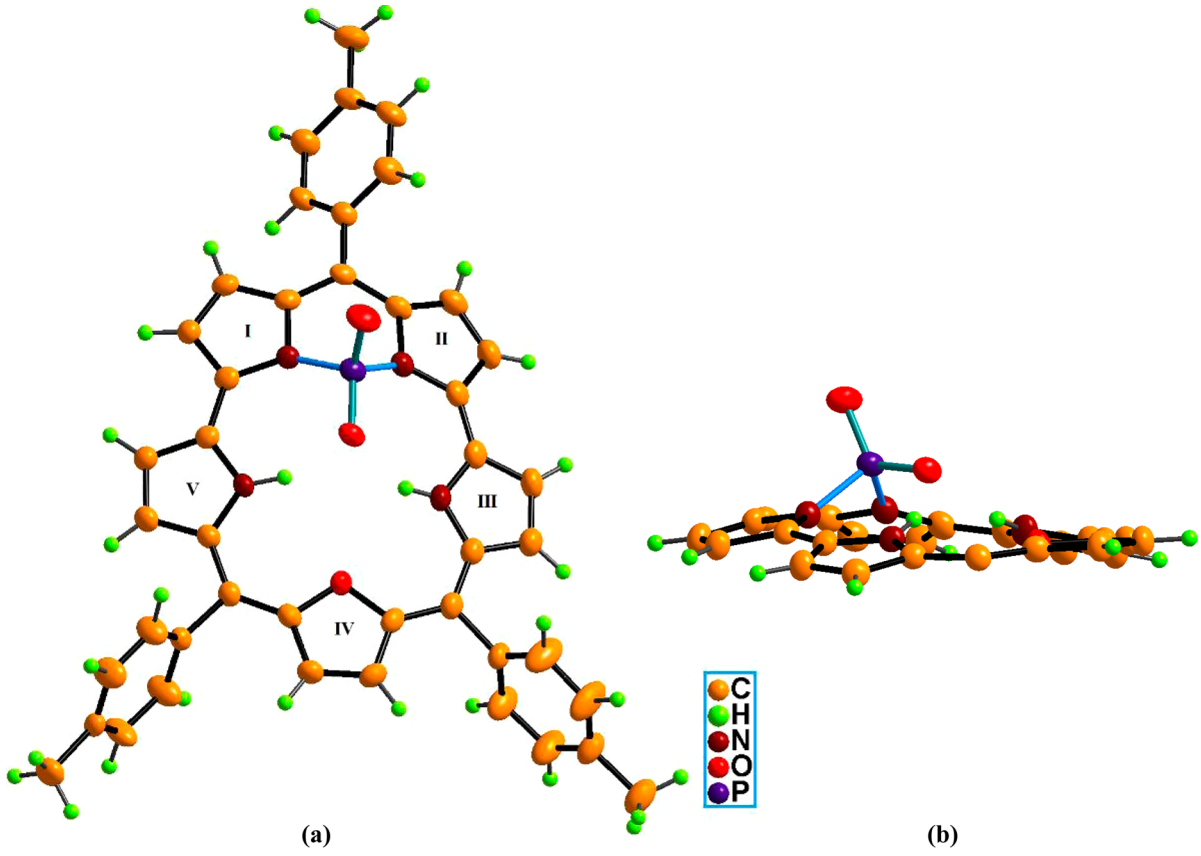

Figure 1. ORTEP diagrams of compound **1**: (a) perspective view; (b) side view (the *meso*-tolyl groups are omitted for clarity). The thermal ellipsoids represent 50% probability.

Table 2. Selected Bond Lengths [Å] and Angles [deg] for Compound 1

P1−N1	1.724(3)
P1−N2	1.726(3)
P1−O1	1.468(3)
P1−O2	1.488(2)
N3−H···O2	1.765
N3−H···O3	2.608
N4−H···O2	1.855
N4−H···O3	2.574
O1−P1−O2	121.42(15)
N1−P1−N2	93.38(14)
N2−P1−O2	109.21(14)
N1−P1−O2	109.97(14)
N1−P1−O1	108.94(16)
N2−P1−O1	110.31(15)

quantum yields of compounds **1**−**4**. Thus, PO_2 complexation of smaragdyrin alters the electronic properties of the macrocycle, as reflected in their photophysical and electrochemical properties.

BODIPY−PO_2-Smaragdyrin Dyad 9. Because the PO_2-smaragdyrins are decently fluorescent and emit at ∼715 nm, they can be used as energy acceptors upon linking with a proper energy donor. We designed and synthesized a covalently linked BODIPY-PO_2-smaragdyrin dyad **9** (Scheme 2). The covalently linked BODIPY-smaragdyrin dyad **10** was prepared by coupling of 4,4-difluoro-8-(4-ethynylphenyl)-4-bora-3a,4a-diaza-*s*-indacene (**11**; BODIPY-CCH) with a 5,10-(4-methylphenyl)-19-(4-iodophenyl)-25-oxasmaragdyrin (**8**) building block in toluene/triethylamine (3:1) in the presence of a catalytic amount of $Pd_2(dba)_3/AsPh_3$ at 40−50 °C for 2 h followed by column chromatographic purification on silica gel. The PO_2 insertion was carried out by treating dyad **10** with $POCl_3$ under reaction conditions similar to those used for the preparation of compounds **1**−**4**, and the resulting crude compound was purified by column chromatography using silica gel to afford compound **9** in 20% yield. Compound **9** was confirmed by HR-MS and ^{1}H, ^{31}P, ^{19}F, and ^{11}B NMR spectroscopy. Compound **9** showed the absorption features

Table 3. Photophysical Data of Compounds 1−5 Recorded in $CHCl_3$ (ε = Extinction Coefficient)

compd	Soret bands (nm) (log ε)		Q bands (nm) (log ε)				λ_{em} (nm)	Φ_f	τ (ns)
1	448 (5.7)	486 (5.3)	611 (4.2)	640 (4.1)	667 (4.5)	708 (4.9)	714	0.18	4.3
2	449 (5.8)	486 (5.4)	611 (4.3)	642 (4.2)	667 (4.5)	708 (4.9)	717	0.19	4.1
3	450 (5.7)	487 (5.4)	612 (4.2)	642 (4.1)	667 (4.5)	709 (4.8)	720	0.15	3.9
4	447 (5.7)	485 (5.3)	611 (4.2)	641 (4.2)	666 (4.4)	707 (4.7)	715	0.13	4.0
5	447 (5.3)		555 (4.2)	600 (4.3)	636 (4.3)	699 (4.2)	710	0.07	3.5

dx.doi.org/10.1021/ic501629n | *Inorg. Chem.* 2014, 53, 9431−9438

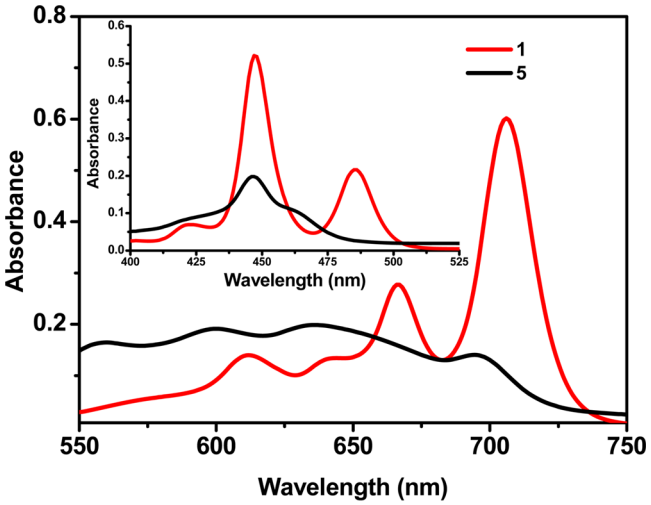

Figure 2. Comparison of the Q and Soret bands (inset) of absorption spectra of the PO_2-smaragdyrin complex **1** and free base smaragdyrin **5** recorded in chloroform. The concentrations used were 10^{-5} and 10^{-6} M for the Q and Soret bands, respectively.

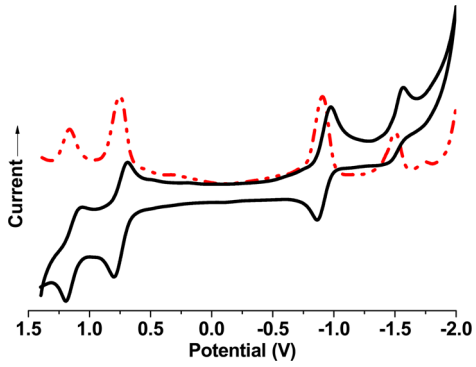

Figure 3. Cyclic voltammogram of compound **1** recorded in CH_2Cl_2 containing 0.1 M TBAP as the supporting electrolyte and using a scan rate of 50 mV s^{-1}. The dotted line represents the DPV curve.

Table 4. Electrochemical Redox Data (V) of Compounds 1–5 Recorded in Dichloromethane Containing 0.1 M TBAP as the Supporting Electrolyte Recorded Using a Scan Rate of 50 mV s^{-1} [a]

	E_{ox} (V)		E_{red} (V)	
compd	I	II	I	II
1	0.74	1.12	−0.92	−1.50
2	0.73	1.11	−0.93	−1.53
3	0.75	1.07	−0.89	−1.45
4	0.84	1.22	−0.83	−1.23
5	0.36	0.72	−1.33	−1.69

[a] $E_{1/2}$ values reported are relative to SCE.

of both BODIPY and PO_2-smaragdyrin units with negligible shifts in their absorption maxima compared to its constituted monomers, indicating that the moieties interact weakly with each other in dyad **9**. The steady-state fluorescence spectra of dyad **9** along with a 1:1 mixture of constituted monomers were recorded using an excitation wavelength of 505 nm, where the BODIPY unit absorbs strongly and is presented in Figure 6. As is clear from Figure 6, in a 1:1 mixture, upon excitation at 505 nm where BODIPY absorbs strongly, the emission was noted

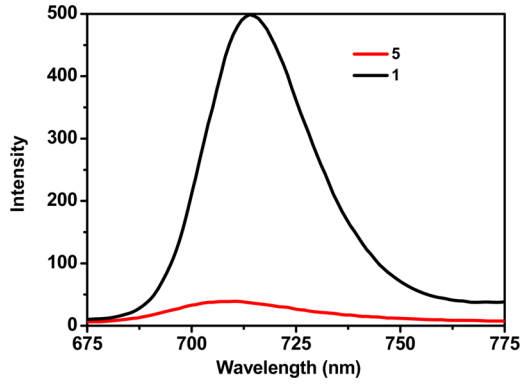

Figure 4. Comparison of emission spectra of the PO_2-smaragdyrin complex **1** and the free base smaragdyrin **5** recorded in chloroform by excitation at their corresponding Soret band maxima.

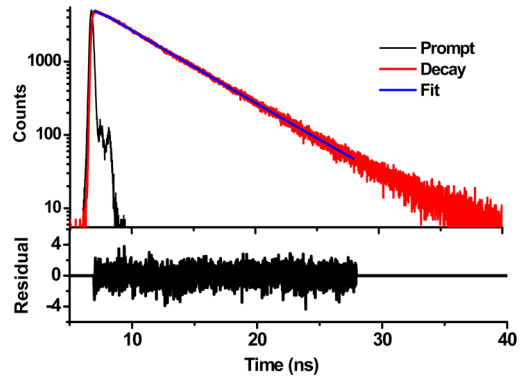

Figure 5. Fluorescence decay profile and weighted residual distribution fits of compound **1** in $CHCl_3$. The excitation wavelength used was 440 nm, and emission was detected at their corresponding wavelengths.

mainly at 525 nm corresponding to the BODIPY unit, with the weak emission at 715 nm corresponding to the PO_2-smaragdyrin unit. However, in dyad **9**, upon excitation at 505 nm, emission from the BODIPY unit was completely quenched and a strong emission was noted from the PO_2-smaragdyrin unit at 720 nm. This indicates that there is an efficient energy-transfer possibility from the donor BODIPY unit to the acceptor PO_2-smaragdyrin unit in dyad **9**. Thus, the PO_2 smaragdyrin unit can act as an efficient energy acceptor upon linking with suitable energy donor moieties.

CONCLUSIONS

In summary, we synthesized the first examples of stable PO_2 complexes of *meso*-triaryl-25-oxasmaragdyrin under reflux conditions. The binding mode of a phosphorus(V) ion with a smaragdyrin macrocycle is completely different from that of other phosphorus(V) complexes of expanded macrocycles reported in the literature.[13−15] PO_2 complexation of a smaragdyrin macrocycle significantly alters the electronic properties, which is clearly reflected in the spectral and electrochemical properties. The PO_2 complexes of smaragdyrins absorb and emit strongly in the visible region and are stable under redox conditions and electron-deficient compared to their free base smaragdyrins. We also successfully inserted PO_2 into the smaragdyrin unit of a covalently linked BODIPY–smaragdyrin dyad and showed the possibility of efficient energy transfer from the BODIPY unit to the PO_2-smsragdyrin unit in

dx.doi.org/10.1021/ic501629n | Inorg. Chem. 2014, 53, 9431−9438

Scheme 2. Synthesis of BODIPY−PO_2-Smaragdyrin Dyad 9

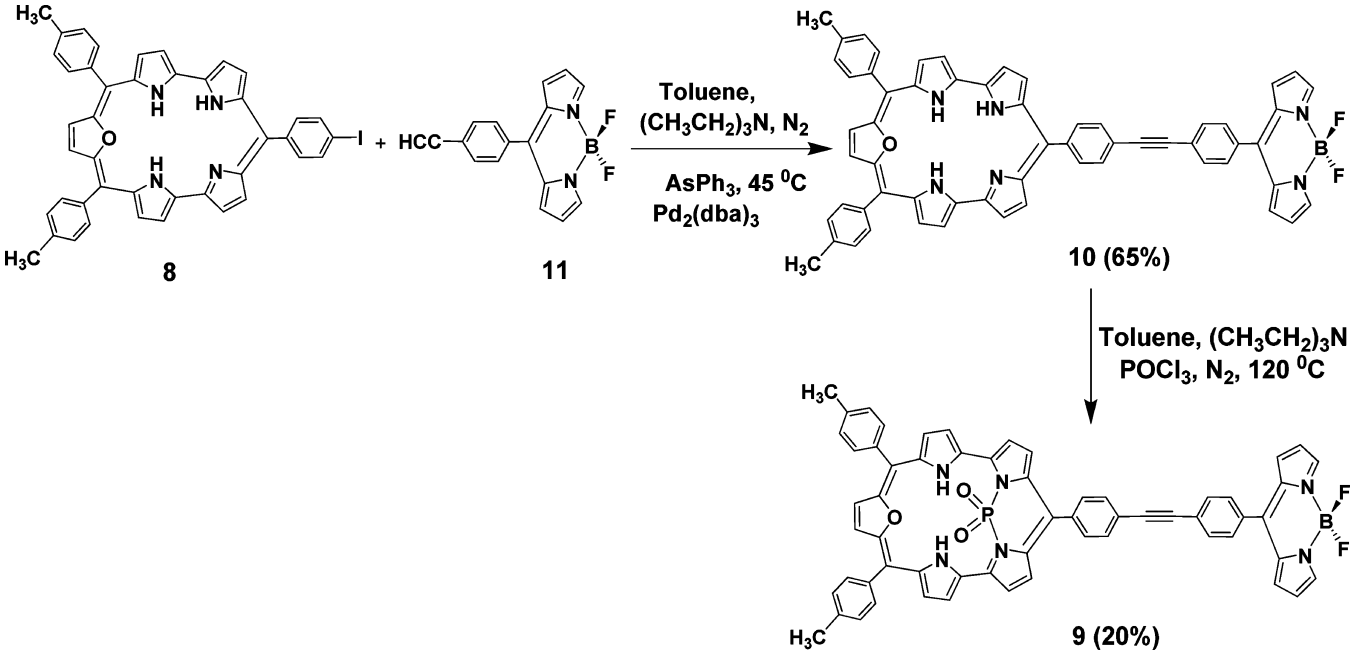

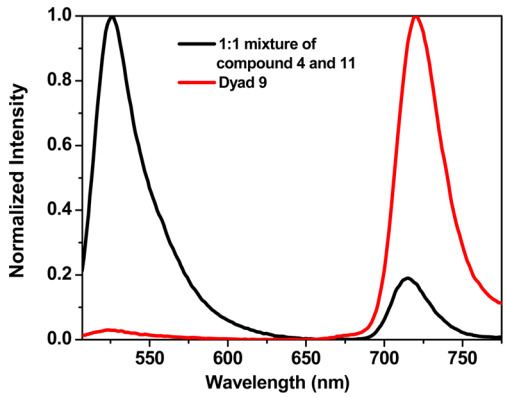

Figure 6. Emission spectra of dyad **9** and a 1:1 mixture of **4** and **11** recorded in a $CHCl_3$ solvent by excitation at 505 nm. The dyad emission profile shows that emission is observed mainly from the PO_2-smaragdyrin unit.

the BODIPY−PO_2-smaragdyrin dyad. Currently, the reactivity of PO_2 complexes of smaragdyrins is under investigation.

EXPERIMENTAL SECTION

General Procedures. Chemicals such as BF_3, Et_2O, TFA, $POCl_3$, PBr_3, PCl_3, and 2,3-dichloro-5,6-dicyano-1,4-benzoquinone were used as obtained from Aldrich. All other chemicals used for the synthesis were reagent grade unless otherwise specified. Column chromatography was performed on silica (60−120 mesh) and basic alumina. The ^1H, ^{13}C, ^{19}F, ^{11}B, and ^{31}P NMR spectra were recorded on a Bruker 400 or 500 MHz instrument using a $CDCl_3$ solvent. The ^1H nucleus has a frequency of 400 MHz, the ^{13}C nucleus 100 MHz, the ^{31}P nucleus 161.8 MHz, the ^{19}F nucleus 470.54 MHz, and the ^{11}B nucleus 160.46 MHz. Tetramethylsilane $[Si(CH_3)_4]$ was used as an internal standard for ^1H and ^{13}C NMR, 85% H_3PO_4 as an external standard for ^{31}P NMR, trifluorotoluene as an external standard for ^{19}F NMR, and boric acid as an external standard for ^{11}B NMR. $^1H-^1H$ COSY and NOESY experiments were performed on Bruker 400 and 500 MHz instruments. Absorption and steady-state fluorescence spectra were obtained with Perkin-Elmer Lambda-35 and PC1 photon counting spectrofluorometers manufactured by ISS and USA instruments, respectively. The fluorescence quantum yields (Φ_f) were estimated from the emission and absorption spectra by a comparative method at an excitation wavelength of 420 nm using H_2TTP (Φ_f = 0.11) as the standard. The time-resolved fluorescence decay measurements were carried out at magic angle using a picosecond diode-laser-based TCSPC fluorescence spectrometer from IBH, U.K. All decays were fitted as single exponential. The good fit criteria were low χ^2 (1.0) and random distributions of residuals. CV studies were carried out with a BAS electrochemical system utilizing the three-electrode configuration consisting of glassy carbon (working electrode), platinum wire (auxiliary electrode), and saturated calomel (reference electrode) electrodes. The experiments were done in dry CH_2Cl_2 using 0.1 M TBAP as the supporting electrolyte. Half-wave potentials were measured using DPV and also calculated manually by taking the average of the cathodic and anodic peak potentials. All potentials were calibrated versus saturated calomel electrode (SCE) by the addition of ferrocene as an internal standard, taking $E_{1/2}(Fc/Fc^+)$ = 0.42 V versus SCE.[16] The HR-MS spectra were recorded with a Bruker maXis Impact mass spectrometer by using the electrospray ionization method and a quadrupole analyzer.

X-ray Crystallography Method. Single crystals of suitable size for a X-ray diffractometer were selected under a microscope and mounted on the tip of a glass fiber, which was positioned on a copper pin. The X-ray data for compound **1** (CCDC 975030) were collected on a Bruker Kappa CCD diffractometer, employing graphite-monochromated Mo Kα radiation at 200 K and the $\theta-2\theta$ scan mode. The space group for compound **1** was determined on the basis of systematic absences and intensity statistics, and the structure of compound **1** was solved by direct methods using *SIR92* or *SIR97* and refined with *SHELXL-97*.[17] An empirical absorption correction by multiscans was applied. All non-hydrogen atoms were refined with anisotropic displacement factors. Hydrogen atoms were placed in ideal positions and fixed with relative isotropic displacement parameters. Detailed crystallographic information for compound **1** is provided in the Supporting Information (CIF).

Procedure for Compounds 1−4. *meso*-Triaryl-25-oxasmaragdyrin **5** (60 mg, 0.0946 mmol) was taken in a round-bottomed flask, and N_2 gas was purged for 5 min. Toluene (20 mL) and triethylamine (0.132 mL, 0.946 mmol) were added to the round-bottomed flask, and N_2 gas purging was continued for an additional 10 min. $POCl_3$ (0.176 mL, 1.892 mmol) was then added, and the reaction mixture was refluxed at 120 °C for 18 h. The reaction was quenched by the

dx.doi.org/10.1021/ic501629n | Inorg. Chem. 2014, 53, 9431−9438

addition of water, and the compound was extracted with CH_2Cl_2. The combined organic layers were washed thoroughly with water and dried over Na_2SO_4. Purification of the crude compound was done by silica gel column chromatography using petroleum ether/CH_2Cl_2 (1:1) as the eluent, and compound **1** was collected as a green solid. The same procedure was followed for compounds **2**–**4**.

Compound 1. Yield: 55%. Mp: >300 °C. ^{1}H NMR (400 MHz, $CDCl_3$, δ in ppm): −1.69 (s, 2H, −NH), 2.76 (s, 3H, $-CH_3$), 2.80 (s, 6H, $-CH_3$), 7.72 (d, 4H, ^3J(H,H) = 8.3 Hz, Ar), 7.79 (d, 2H, ^3J(H,H) = 7.8 Hz, Ar), 8.38 (d, 4H, ^3J(H,H) = 8.3 Hz, Ar), 8.50 (d, 2H, ^3J(H,H) = 7.9 Hz, Ar), 9.27 (dd, 2H, ^3J(H,H) = 4.2 Hz, ^4J(NH,H) = 2.6 Hz, py), 9.63 (dd, 2H, ^3J(H,H) = 4.2 Hz, ^4J(P,H) = 3.0 Hz, py), 9.72 (s, 2H, fur), 10.38–10.40 (m, 4H, py). ^{13}C NMR (100 MHz, $CDCl_3$, δ in ppm): 21.8, 21.8, 108.5, 121.5, 121.5, 122.2, 123.0, 125.2, 125.9, 126.2, 128.4, 129.5, 130.6, 131.7, 134.4, 134.8, 135.5, 138.4, 138.6, 139.2, 139.6, 150.4. ^{31}P{^{1}H} NMR (161.8 MHz, $CDCl_3$, δ in ppm): −32.8. UV–vis [in $CHCl_3$, λ_{max}/nm (log ε)]: 448 (5.72), 486 (5.43), 611 (4.14), 640 (4.12), 667 (4.44), 707 (4.78). HR-MS. Calcd for $C_{44}H_{33}N_4O_3NaP$ [$(M + Na)^+$]: m/z 719.2194. Obsd: m/z 719.2182.

Compound 2. Yield: 57%. Mp: >300 °C. ^{1}H NMR (400 MHz, $CDCl_3$, δ in ppm): −1.65 (s, 2H, −NH), 2.81 (s, 6H, $-CH_3$), 4.17 (s, 3H, $-OCHH_3$), 7.50 (d, 2H, ^3J(H,H) = 8.7 Hz, Ar), 7.72 (d, 4H, ^3J(H,H) = 7.7 Hz, Ar), 8.33 (d, 4H, ^3J(H,H) = 7.3 Hz, Ar), 8.52 (d, 2H, ^3J(H,H) = 7.9 Hz, Ar), 9.24 (dd, 2H, ^3J(H,H) = 4.4 Hz, ^4J(NH,H) = 2.5 Hz, py), 9.61 (dd, 2H, ^3J(H,H) = 4.3 Hz, ^4J(P,H) = 3.0 Hz, py), 9.69 (s, 2H, fur), 10.36–10.39 (m, 4H, py). ^{13}C NMR (100 MHz, $CDCl_3$, δ in ppm): 21.8, 55.9, 108.5, 111.8, 114.3, 121.5, 122.1, 123.0, 125.1, 125.9, 126.2, 128.4, 130.7, 131.7, 134.8, 135.6, 138.4, 139.3, 139.6, 142.5, 150.4, 160.0. ^{31}P{^{1}H} NMR (161.8 MHz, $CDCl_3$, δ in ppm): −32.8. UV–vis [in $CHCl_3$, λ_{max}/nm (log ε)]: 449 (5.80), 486 (5.42), 611 (4.25), 642 (4.24), 667 (4.53), 708 (4.87). HR-MS. Calcd for $C_{44}H_{33}N_4O_4NaP$ [$(M + Na)^+$]: m/z 735.2132. Obsd: m/z 735.2117.

Compound 3. Yield: 45%. Mp: >300 °C. ^{1}H NMR (400 MHz, $CDCl_3$, δ in ppm): −1.63 (s, 2H, −NH), 4.17 (s, 3H, $-OCH_3$), 4.19 (s, 6H, $-OCH_3$), 7.44 (d, 4H, ^3J(H,H) = 8.5 Hz, Ar), 7.50 (d, 2H, ^3J(H,H) = 8.6 Hz, Ar), 8.36 (d, 4H, ^3J(H,H) = 8.0 Hz, Ar), 8.52 (d, 2H, ^3J(H,H) = 8.0 Hz, Ar), 9.24 (dd, 2H, ^3J(H,H) = 4.3 Hz, ^4J(NH,H) = 2.6 Hz, py), 9.61 (dd, 2H, ^3J(H,H) = 4.3 Hz, ^4J(P,H) = 3.0 Hz, py), 9.70 (s, 2H, fur), 10.36–10.38 (m, 4H, py). ^{13}C NMR (100 MHz, $CDCl_3$, δ in ppm): 53.6, 55.9, 108.1, 113.2, 114.3, 121.4, 121.5, 122.1, 123.0, 125.1, 125.8, 126.3, 128.3, 130.7, 131.9, 135.0, 135.6, 136.0, 143.5, 150.6, 160.1, 160.4. ^{31}P{^{1}H} NMR (161.8 MHz, $CDCl_3$, δ in ppm): −32.8. UV–vis [in $CHCl_3$, λ_{max}/nm (log ε)]: 450 (5.72), 487 (5.34), 612 (4.21), 642 (4.18), 667 (4.46), 709 (4.79). HR-MS. Calcd for $C_{44}H_{33}N_4O_6NaP$ [$(M + Na)^+$]: m/z 767.2030. Obsd: m/z 767.2036.

Compound 4. Yield: 38%. Mp: >300 °C. ^{1}H NMR (400 MHz, $CDCl_3$, δ in ppm): −1.84 (s, 2H, −NH), 2.82 (s, 6H, $-CH_3$), 7.72 (d, 4H, ^3J(H,H) = 7.7 Hz, Ar), 8.32–8.35 (m, 8H, Ar), 9.29 (dd, 2H, ^3J(H,H) = 4.4 Hz, ^4J(NH,H) = 2.6 Hz, py), 9.58 (d, 2H, ^3J(H,H) = 3.4 Hz, py), 9.74 (s, 2H, fur), 10.40–10.42 (m, 4H, py). ^{13}C NMR (100 MHz, $CDCl_3$, δ in ppm): 21.8, 95.5, 108.9, 121.8, 122.3, 122.4, 125.6, 126.0, 126.5, 128.4, 129.2, 131.8, 134.9, 136.1, 136.5, 137.9, 138.5, 138.9, 139.5, 150.5. ^{31}P{^{1}H} NMR (161.8 MHz, $CDCl_3$, δ in ppm): −33.1. UV–vis [in $CHCl_3$, λ_{max}/nm (log ε)]: 447 (5.71), 485 (5.31), 611 (4.20), 641 (4.16), 666 (4.45), 707 (4.77). HR-MS. Calcd for $C_{43}H_{30}IN_4O_3NaP$ [$(M + Na)^+$]: m/z 831.0992. Obsd: m/z 831.0991.

Compound 9. The same procedure as that for compounds **1**–**4** was used. Yield: 20%. Mp: >300 °C. ^{1}H NMR (400 MHz, $CDCl_3$, δ in ppm): −1.81 (s, 2H, −NH), 2.82 (s, 6H, $-CH_3$), 6.62–6.63 (m, 2H, py), 7.04 (d, 2H, ^3J(H,H) = 4.0 Hz, py), 7.68–7.75 (m, 6H, Ar), 7.88 (d, 2H, ^3J(H,H) = 8.2 Hz, Ar), 8.00 (s, 2H, py), 8.18 (d, 2H, ^3J(H,H) = 8.3 Hz, Ar), 8.35 (d, 4H, ^3J(H,H) = 7.4 Hz, Ar), 8.65 (d, 2H, ^3J(H,H) = 7.8 Hz, Ar), 9.30 (dd, 2H, ^3J(H,H) = 4.5 Hz, ^4J(NH,H) = 2.5 Hz, py), 9.65 (dd, 2H, ^3J(H,H) = 4.4 Hz, ^4J(P,H) = 3.0 Hz, py), 9.75 (s, 2H, fur), 10.42–10.45 (m, 4H, py). ^{31}P{^{1}H} NMR (161.8 MHz, $CDCl_3$, δ in ppm): −33.0. ^{19}F NMR (470.54 MHz, $CDCl_3$, δ in ppm): −144.8 (q, ^1J(B,F) = 28.2 Hz). ^{11}B NMR (160.46 MHz, $CDCl_3$, δ in ppm): 0.4 (t, ^1J(B,F) = 28.5 Hz). UV–vis (in $CHCl_3$, λ_{max}/nm): 450, 486, 509 (sh), 613, 645, 670, 710. HR-MS. Calcd for $C_{60}H_{41}BF_2N_6O_3P$ [$(M + H)^+$]: m/z 973.3043. Obsd: m/z 973.3050.

Compound 10. Compounds **8**[8] (40 mg, 0.0536 mmol) and BODIPY-CCH **11**[18] (15 mg, 0.0536 mmol) were dissolved in dry toluene/triethylamine (3:1) in a 25 mL round-bottomed flask fitted with a reflux condenser and gas inlet and outlet tubes for N_2 purging. The reaction mixture was placed in an oil bath preheated to 45 °C. After purging with N_2 for 15 min, $AsPh_3$ (57 mg, 0.187 mmol) and $Pd_2(dba)_3$ (21 mg, 0.0235 mmol) were added, and the reaction was stirred at 40–50 °C for 2 h. TLC analysis of the reaction mixture indicated the appearance of a major brownish-green new spot. The crude compound was subjected to silica gel chromatography, and the desired compound was collected using petroleum ether/dichloromethane (60:40). The solvent was removed with a rotary evaporator under vacuum and afforded pure compound **10**. Yield: 65%. Mp: >300 °C. ^{1}H NMR (400 MHz, $CDCl_3$, δ in ppm): 2.73 (s, 6H, $-CH_3$), 6.58–6.60 (m, 2H, py), 7.01 (d, 2H, ^3J(H,H) = 4.4 Hz, py), 7.58–7.69 (m, 6H, Ar), 7.84–7.93 (m, 4H, Ar + py), 8.05–8.11 (m, 6H, Ar), 8.42 (d, 2H, ^3J(H,H) = 7.8 Hz, Ar), 8.48 (d, 2H, ^3J(H,H) = 3.9 Hz, py), 8.81 (s, 2H, fur), 8.98 (d, 2H, ^3J(H,H) = 4.0 Hz, py), 9.41 (d, 2H, ^3J(H,H) = 4.0 Hz, py), 9.50 (d, 2H, ^3J(H,H) = 4.2 Hz, py). UV–vis (in $CHCl_3$, λ_{max}/nm): 449, 504, 555, 598, 640, 706. HR-MS. Calcd for $C_{60}H_{41}BF_2N_6O$ [$(M)^+$]: m/z 910.3407. Obsd: m/z 910.3399.

■ ASSOCIATED CONTENT

Ⓢ Supporting Information

X-ray crystallographic data in CIF format and characterization data for all new compounds. This material is available free of charge via the Internet at http://pubs.acs.org.

■ AUTHOR INFORMATION

Corresponding Author

*E-mail: ravikanth@chem.iitb.ac.in.

Notes

The authors declare no competing financial interest.

■ ACKNOWLEDGMENTS

We thank the Department of Science & Technology, Government of India, for financial support, and H.K. thanks the CSIR for a fellowship.

■ REFERENCES

(1) Pareek, Y.; Ravikanth, M.; Chandrashekar, T. K. *Acc. Chem. Res.* **2012**, *45*, 1801–1816.

(2) Sessler, J. L.; Davis, J. M. *Acc. Chem. Res.* **2001**, *34*, 989–997.

(3) Sessler, J. L.; Tomat, E. *Acc. Chem. Res.* **2007**, *40*, 371–379.

(4) (a) Woodward, R. B. Aromaticity. *An International Symposium*, Sheffield, U.K., 1966; The Chemical Society: London, 1966; Special Publication No. 21. (b) Broadhurst, M. J.; Grigg, R.; Johnson, A. W. *J. Chem. Soc., Perkin Trans. 1* **1972**, 2111–2116.

(5) Sessler, J. L.; Davis, J. M.; Lynch, V. *J. Org. Chem.* **1998**, *63*, 7062–7065.

(6) Narayanan, S. J.; Sridevi, B.; Chandrashekar, T. K. *Org. Lett.* **1999**, *1*, 587–590.

(7) Sridevi, B.; Narayanan, S. J.; Rao, R.; Chandrashekar, T. K. *Inorg. Chem.* **2000**, *39*, 3669–3677.

(8) Rao, M. R.; Ravikanth, M. *J. Org. Chem.* **2011**, *76*, 3582–3587.

(9) Kalita, H.; Lee, W.-Z.; Ravikanth, M. *Dalton Trans.* **2013**, *42*, 14537–14544.

(10) (a) Carrano, C. J.; Tsutsui, M. *J. Coord. Chem.* **1977**, *7*, 79. (b) Mangani, S.; Meyer, E. F.; Cullen, D. L.; Tsutsui, M.; Carrano, C. J. *Inorg. Chem.* **1983**, *22*, 400–404. (c) Marrese, C. A.; Carrano, C. J. *Inorg. Chem.* **1983**, *22*, 1858–1862.

(11) (a) Ghosh, A.; Ravikanth, M. *Chem.—Eur. J.* **2012**, *18*, 6386–6396. (b) Liang, X.; Mack, J.; Zheng, L.-M.; Shen, Z.; Kobayashi, N.

Inorg. Chem. **2014**, *53*, 2797−2802. (c) Simkhovich, L.; Mahammed, A.; Goldberg, I.; Gross, Z. *Chem.—Eur. J.* **2001**, *7*, 1041−1055. (d) Ghosh, A.; Lee, W.-Z.; Ravikanth, M. *Eur. J. Inorg. Chem.* **2012**, 4231−4239.
(12) Młodzianowska, A.; Latos-Grazyński, L.; Szterenberg, L. *Inorg. Chem.* **2008**, *47*, 6364−6374.
(13) Miura, T.; Higashino, T.; Saito, S.; Osuka, A. *Chem.—Eur. J.* **2010**, *16*, 55−59.
(14) Higashino, T.; Lim, J. M.; Miura, T.; Saito, S.; Shin, J.-Y.; Kim, D.; Osuka, A. *Angew. Chem., Int. Ed.* **2010**, *49*, 4950−4954.
(15) Higashino, T.; Osuka, A. *Chem. Sci.* **2012**, *3*, 103−107.
(16) Masui, M.; Sayo, H.; Tsuda, Y. *J. Chem. Soc. B* **1968**, 973−976.
(17) Sheldrick, G. M. *Acta Crystallogr., Sect. A* **2008**, *A64*, 112. *Program for Crystal Structure Solution and Refinement*; University of Goettingen: Goettingen, Germany, 1997.
(18) Burghart, A.; Thoresen, L. H.; Chen, J.; Burgess, K.; Bergstrom, F.; Johansson, L. B. A. *Chem. Commun.* **2000**, 2203−2204.